



EEG Functional Connectivity Underlying Emotional Valence and Arousal Using Minimum Spanning Trees

Rui Cao^{1*}, Yan Hao¹, Xin Wang², Yuan Gao², Huiyu Shi¹, Shoujun Huo¹, Bin Wang², Hao Guo² and Jie Xiang²

¹ College of Software Engineering, Taiyuan University of Technology, Taiyuan, China, ² College of Computer Science and Technology, Taiyuan University of Technology, Taiyuan, China

OPEN ACCESS

Edited by:

Xi-Nian Zuo,
Beijing Normal University, China

Reviewed by:

Qi Li,
Changchun University of Science
and Technology, China
HaoMing Dong,
Yale University, United States

*Correspondence:

Rui Cao
caorui@tyut.edu.cn

Specialty section:

This article was submitted to
Brain Imaging Methods,
a section of the journal
Frontiers in Neuroscience

Received: 19 December 2019

Accepted: 24 March 2020

Published: 07 May 2020

Citation:

Cao R, Hao Y, Wang X, Gao Y,
Shi H, Huo S, Wang B, Guo H and
Xiang J (2020) EEG Functional
Connectivity Underlying Emotional
Valence and Arousal Using Minimum
Spanning Trees.
Front. Neurosci. 14:355.
doi: 10.3389/fnins.2020.00355

In recent years, traditional methods such as power spectrum and amplitude analysis have been used to research the emotional electroencephalogram (EEG). The brain network method is also used in emotional EEG research, which can better reflect the activity of brains. A minimum spanning tree (MST) represents the key information flow in the weighted brain network, and it provides a sensitive method to capture subtle information in network organization while effectively avoiding the shortcomings of traditional brain networks. The DEAP dataset provides electroencephalogram (EEG) data for four categories of emotions: high arousal and high valence (HAHV), high arousal and low valence (HALV), low arousal and high valence (LAHV), and low arousal and low valence (LALV). Phase lag index (PLI) weighted matrices were calculated in five frequency bands. On this basis, the minimum spanning trees were constructed. At the same valence level in the gamma (γ) band, HAHV and HALV showed significant higher mean PLI (MPLI), maximum degree (Degree_{\max}) and leaf fraction and significant lower diameter and eccentricity than LAHV and LALV. At the same arousal level in the γ band, HALV showed significant higher MPLI, Degree_{\max} and leaf fraction and significant lower diameter and eccentricity than HAHV. These results indicate that the low-arousal showed more line-shaped configurations than the high-arousal. Additionally, in the high-arousal condition, a shift toward more star-shaped trees from high-valence to low-valence supports the trend toward randomness of the brain network with negative emotions and that the brain is more activated when faced with negative emotions. From a brain network perspective, this phenomenon provides a theoretical basis for negative bias.

Keywords: emotion, negative bias, functional connectivity, graph theory, minimum spanning tree

INTRODUCTION

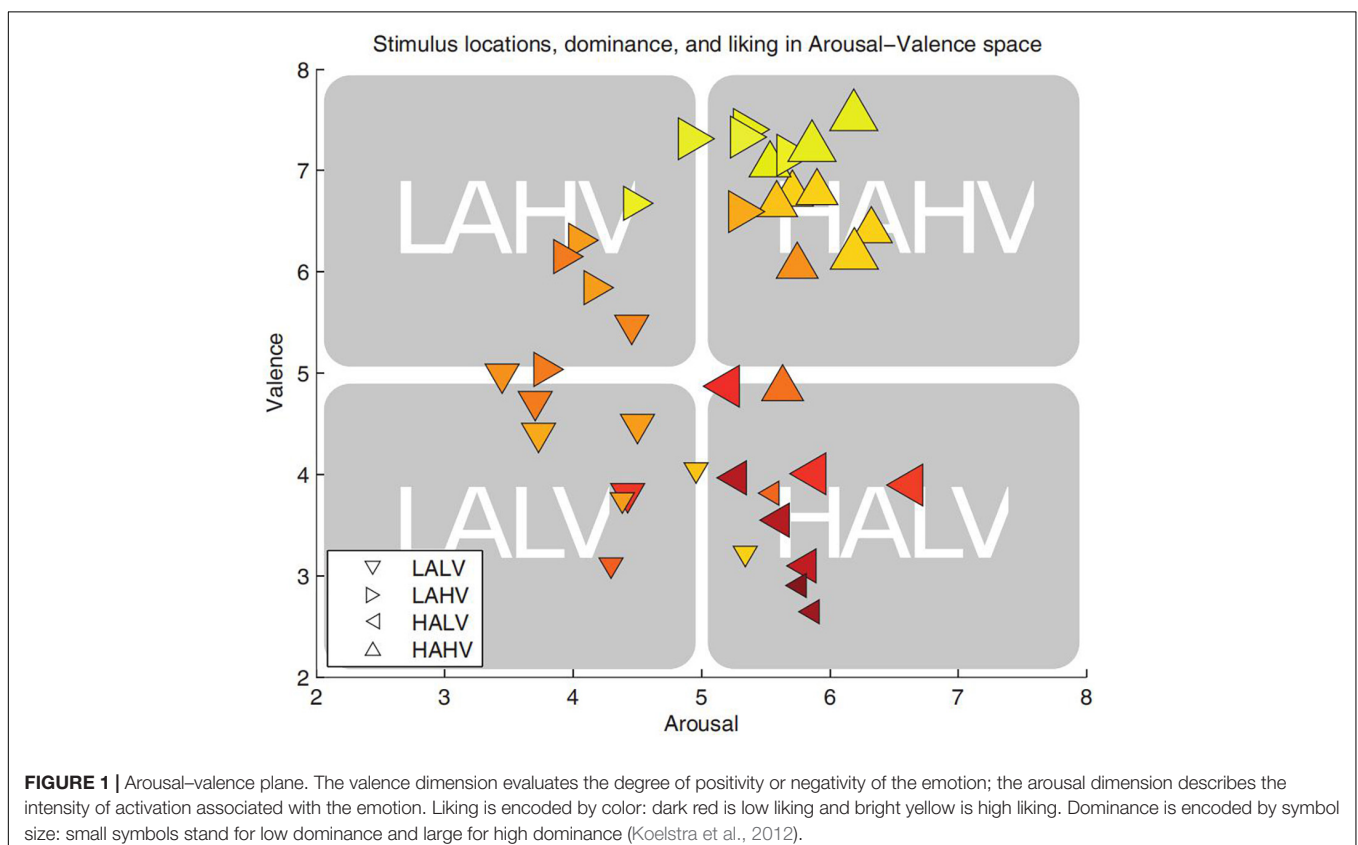
Emotion processing is one of the advanced cognitive functions of the human brain. Increasing attention has been paid to the study of the influence of different emotions on the human brain. Electroencephalogram (EEG) and event-related potential (ERP) recording can capture and assess neural responses to affective events with a high temporal resolution and are widely

used in emotional research. In general, affective content can produce stronger emotional effects than neutral content can (Olofsson et al., 2008). Many studies have demonstrated this using synchronicity (Zhang et al., 2012), amplitude (Pegg et al., 2019) and other characteristics. Furthermore, some studies find that bad moods have a larger impact than good moods and that events involving unpleasant emotions remain more salient in people's minds than events involving pleasant emotions do (Baumeister et al., 2001; Amrisha et al., 2008). When studying emotional facial expression, Li found that the coherence of negative emotion was greater than that of positive emotion in both the low and high γ bands (Li et al., 2015). Zhu L found that the phase lock value of positive video stimulation was significantly lower than that of negative stimulation in the β and γ bands (Zhu et al., 2018).

At present, traditional EEG analysis methods, including methods that focus on the power spectrum (Liu et al., 2018), coherence (Zhang et al., 2012; Mu et al., 2017) and phase lock value (Zhu et al., 2018), are widely used. The brain regions coordinate and cooperate with each other to form a complex brain network, and the development of graph theory provides a perfect tool for brain network analysis (Rubinov and Sporns, 2010; Calhoun et al., 2018). Graph theory can sensitively capture subtle changes in the network and has revealed fundamental mechanisms of functional brain organization in EEG analysis (Fraschini et al., 2016). Li used traditional graph theory to find that the number of active brain network connections

during negative stimuli was greater than the number of active connections during positive stimuli (Li et al., 2015). These results concerning topological structure provided new evidence that healthy controls had a negative bias in terms of the functional connectivity of brain networks.

Although traditional graph theory provides a new perspective and means of discovery in brain network analysis, the methodology used in traditional graph theory has some problems that cause the same research conditions to result in different—or even opposite—conclusions (Tijms et al., 2013; van Diessen et al., 2015). In particular, a traditional unweighted network involves threshold selection but provides no reasonable way to select the threshold. Improper threshold selection may lead to false links or cause the loss of important information (van Wijk et al., 2010). Even the use of weighted rather than unweighted graphs does not provide an optimal solution because measures computed on these graphs are influenced by the large number of noisy connections and by the average functional connectivity strength (Tewarie et al., 2014). However, a minimum spanning tree (MST) effectively avoids the problems of weighted and unweighted brain networks (Eric et al., 2013; Tewarie et al., 2015). An MST connects all nodes in the network without forming a cycle, and it generates the strongest subconnection. The MST represents the key information flow in the weighted network (it includes the high-probability connections of all the shortest paths in the network) (van Dellen et al., 2014). In recent years, scholars have applied the MST method to study



epilepsy (van Diessen et al., 2016), children's brain development (Boersma et al., 2013), motor imagination (Demuru et al., 2013) and other fields. Moreover, compared with traditional network methods, the MST method has superior sensitivity to small differences in the brain network (Demuru et al., 2013; van Diessen et al., 2016), providing a new tool for research on complex brain networks. To date, there have been few reports on using an MST to analyze the differences between different emotions. The MST method is used in this study to explore the differences in brain network topology when subjects are in different emotional states.

MATERIALS AND METHODS

EEG Data Acquisition

All of the subjects comes from the Dataset for Emotion Analysis using the Physiological and Audiovisual Signals (DEAP) database. The DEAP database is an open database for emotion recognition research based on physiological signals (Koelstra et al., 2012). The database contains EEG data collected from 32 subjects as they watched 40 music videos. These videos had obvious emotional stimulation effects and the duration of each video was 1 min.

Data Preprocessing

The EEG data were acquired from the DEAP data collection website. The raw EEG data were preprocessed in a series of steps that included down-sampling to 128 Hz, electro-oculogram

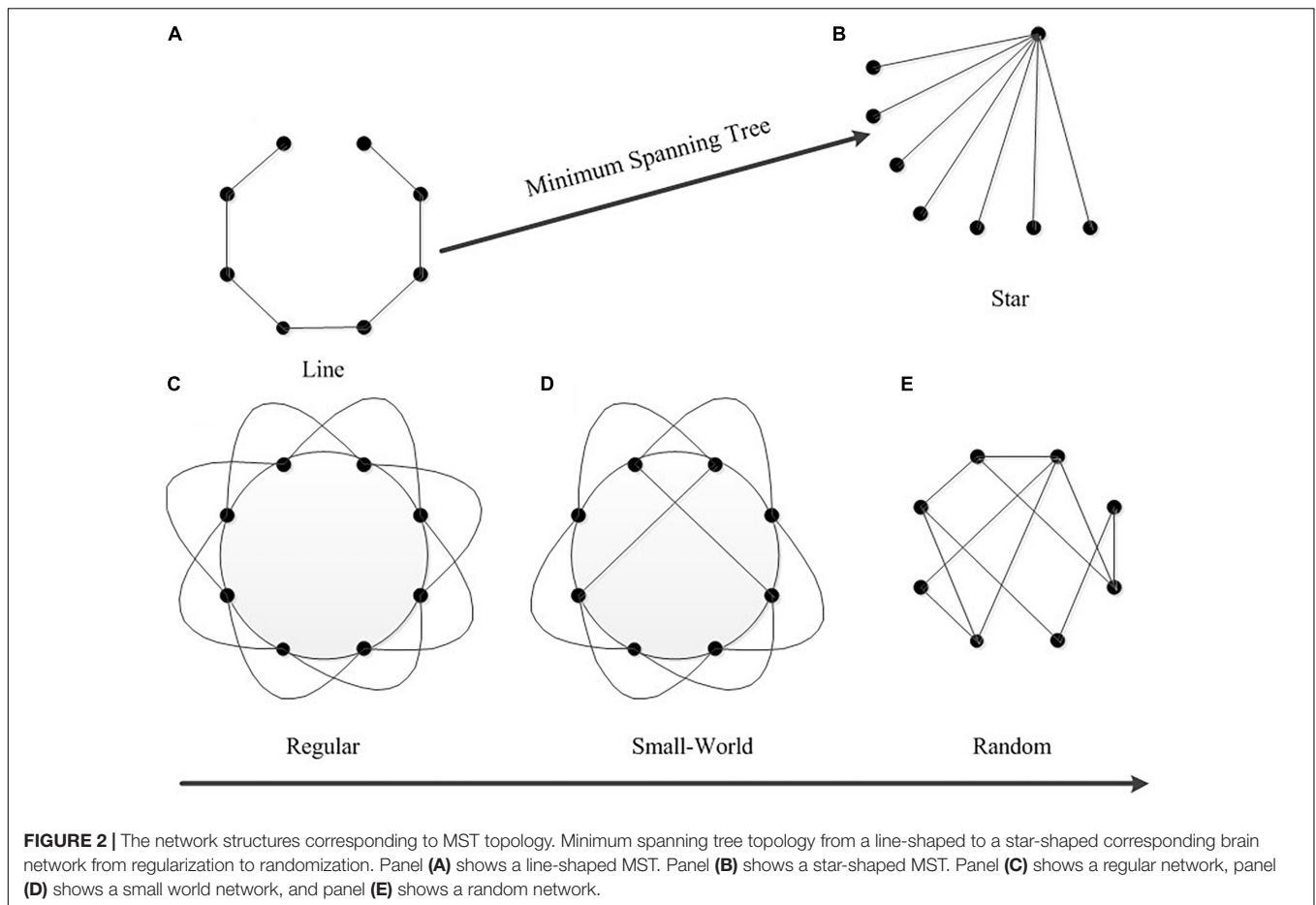
(EOG) removal and filtering at 4.0–45.0 Hz. The length of each sampling period was 63 s and the first 3 s was a baseline period, which was followed by 60 s of EEG data collected as the subject watched a video.

Each video has two VAD (valence, arousal, dominance) values, one from the behavioral experiment and the other provided by the subjects during the EEG acquisition: while they watched the video, the participants evaluated the video in each VAD dimension using a 9-point scale according to their emotional experiences. Arousal ranged from inactive (e.g., uninterested, bored) to active (e.g., alert, excited), whereas valence ranged from unpleasant (e.g., sad, stressed) to pleasant (e.g., happy, elated). Based on the A and V values, these videos were divided into four types: high arousal/high valence (HAHV) meaning happy and excited, low arousal/high valence (LAHV) meaning calm and chill, low arousal/low valence (LALV) meaning sad and depressed and high arousal/low valence (HALV) meaning angry and shocked (Koelstra et al., 2012).

After the online behavior experiment, 40 music videos were selected from 120 videos because the AV value of these 40 videos was more extreme, showing that they provided a better stimulation for emotion (Figure 1). However, a video scoring near one of the coordinate axes could not be accurately classified into one of the selected emotion categories. Thus, in this experiment (Kuai et al., 2017), scores of 1–4 were used as low scores, and scores of 6–9 were used as high scores. In the scoring process, subject number 23 divided the 40 music videos into three categories instead of four, so the EEG data recorded by

TABLE 1 | MST descriptive statistics.

Symbol	Concept	Explanation	Formula
N	Nodes	Number of nodes in MST	–
M	Links	Number of links in the MST	–
k_i	Degree	Number of links for a given node. Degree _{max} represents the maximum of all node degrees. It may be considered a feature of “hubs,” i.e., crucial regions in the functional brain network.	$k_i = \sum_{j \in N} a_{ij}$
L_f	Leaf fraction	Measured based on the leaf number (the number of nodes that have only one connection). In the formula, L represents the total number of leaves of an MST. When the leaf fraction is high, communication is largely dependent on hub nodes.	$L_f = L/M$
D	Diameter	A measure of the efficiency of global network organization. In the formula, d represents the maximum path length in an MST. In a network with a small diameter, information is efficiently processed between remote brain regions.	$D = d/M$
E	Eccentricity	The longest optimal path from a reference node to any other node in the MST, where $d(i,j)$ represents the optimal (shortest) path between node i and node j . The average eccentricity represents the average value of the eccentricity of all nodes. Low average eccentricity means that the nodes of the MST are closer to the hub nodes.	$E_i = \max\{d(i,j) j \in N\}$
BC	Betweenness centrality	Fraction of all shortest paths that pass through a particular node. ρ_{hj} is the number of shortest paths between h and j , and $\rho_{hj}^{(i)}$ is the number of shortest paths between h and j that pass through i . BC _{max} represents the maximum BC value of all nodes of an MST. It describes the importance of the most central node, which is a measure of central network organization.	$BC_i = \frac{1}{(n-1)(n-2)} \sum_{\substack{h,j \in N \\ h \neq i, j \neq i}} \frac{\rho_{hj}^{(i)}}{\rho_{hj}}$
Th	Tree hierarchy	A hierarchical metric that quantifies the trade-off between large scale integration in the MST and central node overloading.	$Th = \frac{L}{2MBC_{max}}$



subject 23 was abandoned and only the remaining subjects' EEG data were retained.

Frequency Division

In the human brain, different neuron oscillation frequencies are closely related to the functional activity of the brain (Fellinger et al., 2011; Groppe et al., 2013). Therefore, EEG signals are often divided into different frequency bands in EEG research. In this experiment, EEG data are analyzed in the following five frequency bands: θ (4–7 Hz), α (7–13 Hz), β_1 (13–20 Hz), β_2 (20–30 Hz) and γ (31–45 Hz).

Constructing a Correlation Matrix and MST

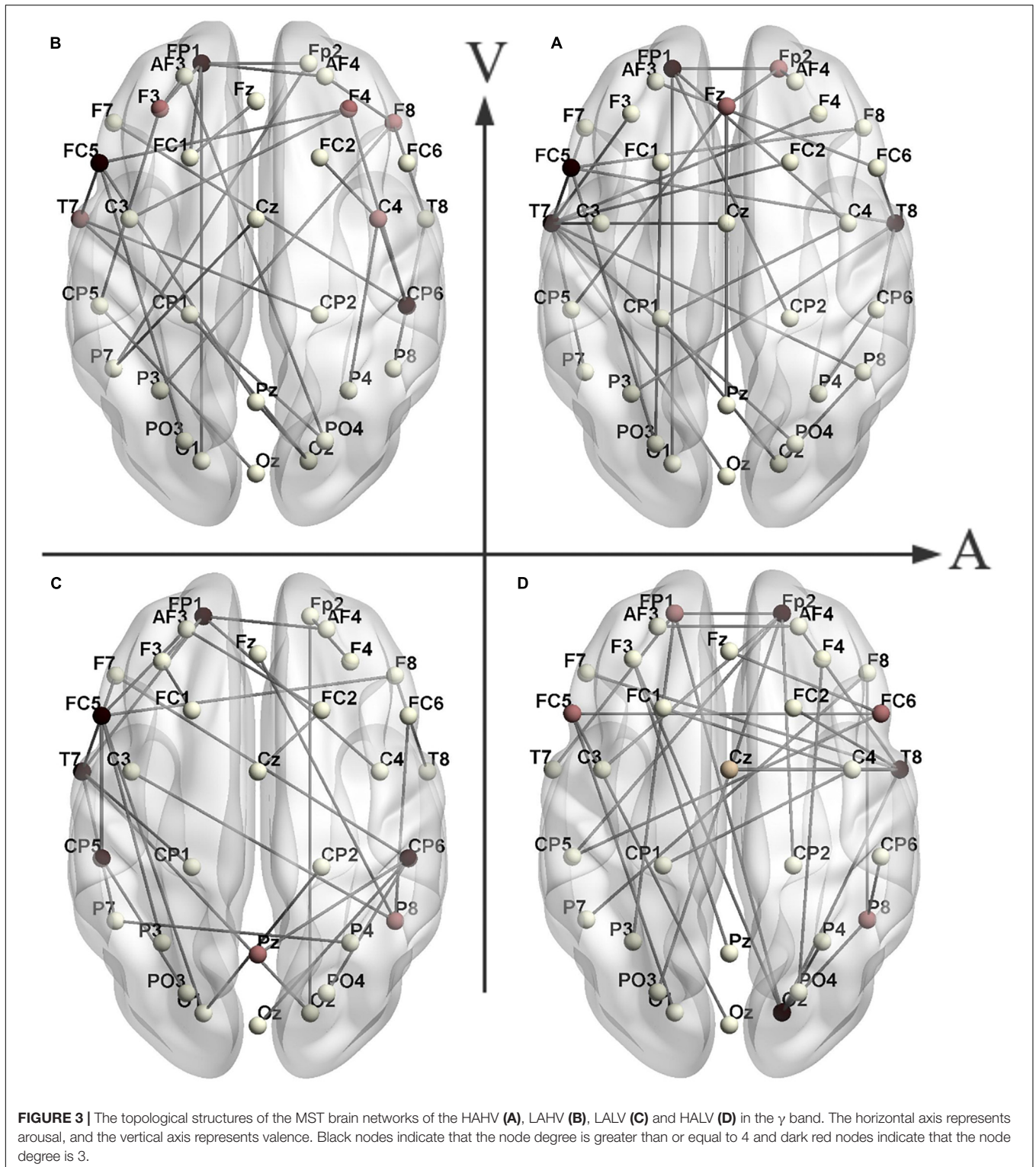
A network consists of nodes and edges. In this experiment, 32 scalp electrodes were used as the nodes of the network, and the phase lag index (PLI) was used for the network edges. The PLI measures the asymmetry of the distribution of phase differences between two signals, and it is relatively insensitive to the confounding effects of volume conduction (Stam et al., 2014). PLI can reflect the consistency with which one signal's phase leads or lags relative to another signal, and it is an effective estimation of phase synchronization (Stam et al., 2007). A 32×32 correlation matrix can be obtained by calculating the PLI value

between each pair of nodes. Whole-brain mean PLI (MPLI) was computed by averaging all the pairwise PLI values, resulting in a single PLI value in order to describe the average functional connectivity for each brain network. Similar methods have been used by Groppe et al. (2013), and the mean synchronization likelihood (SL) was used to characterize the average connection strength of the brain during different emotional stimuli.

For each subject, EEG data was recorded when watching a music video and a PLI matrix was calculated in one frequency band. Then the minimum spanning tree was generated using a Kruskal algorithm (Kruskal, 1956). This procedure started with ranking all connection weights from lowest weight to highest weight. Because we were interested in the strongest connections, we ranked all connections from highest to lowest weight and started by disconnecting all nodes, then added the connection with the highest weight. Next, the connection with the second highest weight was added, and this procedure was repeated until all nodes were connected and it did not form a closed loop. The final MST for each affective brain network contains 32 nodes and 31 edges.

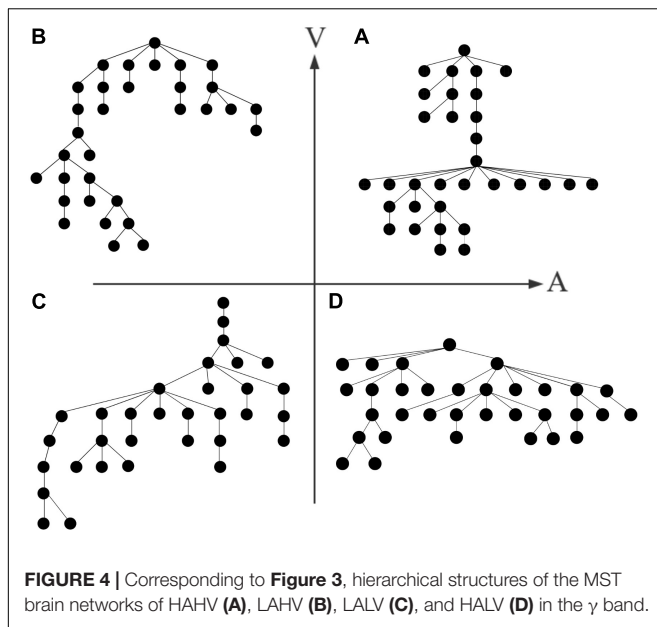
MST Network Metrics

The commonly used characteristics of MST analysis include degree, betweenness centrality (BC), eccentricity, diameter,



leaf fraction and tree hierarchy, among which degree, BC and eccentricity are local attribute values of individual nodes (Table 1). In order to find the eccentricity, the mean value over all nodes was calculated. The maximum values of BC and Degree (BC_{max} and $Degree_{max}$, respectively) are listed

separately. All of the other metrics are global measurements - they characterize the MST as a whole. An important aspect of complex networks is efficient communication between all nodes, which requires a small diameter, i.e., a tree network with a star-shaped topology. In a star-shaped tree, the central node might



easily become overloaded because it has a high BC. An optimal tree configuration should therefore strike a balance between diameter reduction and overload prevention (**Figure 2**). A tree hierarchy measure that captures this trade-off was calculated (Boersma et al., 2013).

The MST can be regarded as the backbone of the brain network and any change in the topological structure of the MST also sensitively reflects change trends in the brain network. An MST with a small degree, small BC, long diameter and few leaves tends to be “line”-shaped. On the contrary, an MST with a large degree, large BC, short diameter and many leaves tends to be “star”-shaped. **Figure 2** shows the network structures corresponding to MST topology. Part A shows an MST with a “line” shape where every node except two end nodes is connected to its two neighbors (low leaf number), but it takes 7 steps to reach the other end of the network (high diameter), and the corresponding network is a regular network. Part B is a “star”-shaped MST which consists of a central node that is connected to other nodes (high degree and BC), which are all leaf nodes (high leaf number). This MST is highly efficient (low diameter) and the corresponding network is a random network. The lower part of **Figure 2** shows the underlying topologies of a regular network, a small world network and a random network, which correspond to MSTs from “line” to “star.” As the topological shape changes from a regular network to a random network, the MST diameter and leaf fraction change according to the path length of the underlying network (the diameter of MST is positively related to the path length, and the leaf fraction of an MST is negatively related to the path length).

RESULTS

For the same emotion, the minimum spanning trees of different subjects overlapped to form a connected graph under the

TABLE 2 | The interaction in the γ band between arousal and valence of repeated measurement analysis of variance.

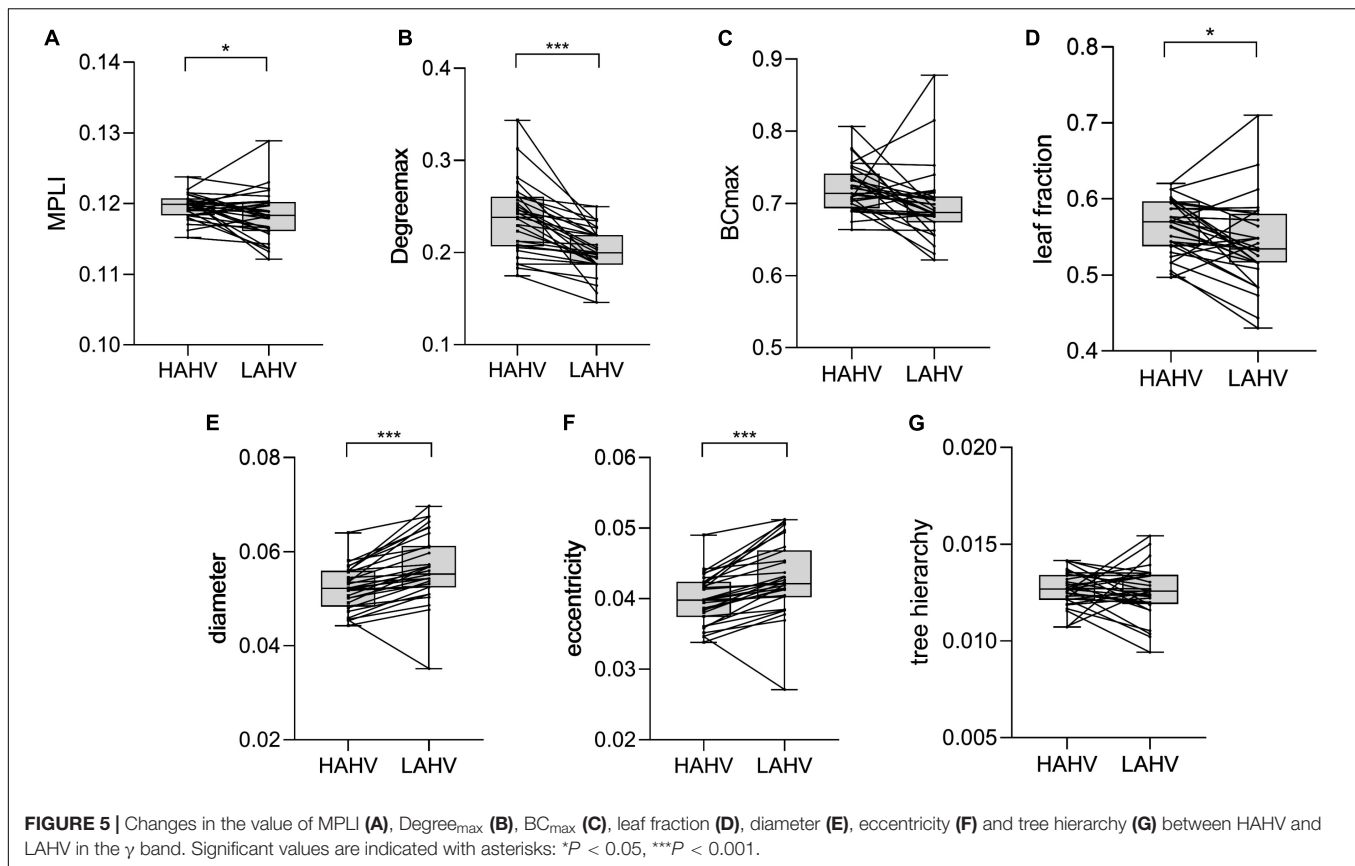
Within-subjects effects characteristic	$F(29,1)$	P	ES
Arousal \times Valence			
MPLI	5.015	0.033	0.614
Degree _{max}	4.423	0.044	0.128
BC _{max}	4.065	0.053	0.119
Leaf fraction	4.443	0.043	0.129
Diameter	4.478	0.043	0.13
Eccentricity	5.213	0.03	0.148
tree Hierarchy	0.008	0.93	0.0002

condition that the same node exists. The weight of the edge in a connected graph means the number of overlapping edges of minimum spanning trees. An MST of the connected graph generated by the Kruskal algorithm is an average minimum spanning tree (average MST) of this emotion. **Figure 3** shows the topological structure of the average MST for the four types of emotions in the γ band, in which the average MST edges mean the edges of maximum weights in the connected graph. **Figure 4** shows the tree hierarchy of the MST corresponding to **Figure 3** for each of the four different emotions in the γ band.

We repeatedly applied an analysis of variance measurement in the 2 (arousal/valence) \times 2 (high/low) within-subject experimental region. The frequency ranges with significant differences were mainly in the γ band (**Table 2**). It was found that there were significant differences in MPLI characteristics under arousal conditions [$F(29,1) = 47.8$,

TABLE 3 | After paired t test and FDR correction, significant changes in MPLI and MST characteristics are seen between emotions in the γ band.

Characteristic	Emotion	Mean \pm SD		t	P
MPLI	HAHV	0.119 \pm 0.0017	HAHV-LAHV	2.326	0.036
	LAHV	0.118 \pm 0.0033	HALV-LALV	5.572	0
	HALV	0.121 \pm 0.0027	HAHV-HALV	-4.752	0
	LALV	0.118 \pm 0.0032	LAHV-LALV	-0.175	0.862
Degree _{max}	HAHV	0.236 \pm 0.037	HAHV-LAHV	6.227	0
	LAHV	0.201 \pm 0.024	HALV-LALV	5.903	0
	HALV	0.27 \pm 0.052	HAHV-HALV	-4.467	0
	LALV	0.214 \pm 0.036	LAHV-LALV	-2.345	0.026
Leaf fraction	HAHV	0.562 \pm 0.035	HAHV-LAHV	2.658	0.016
	LAHV	0.54 \pm 0.056	HALV-LALV	5.218	0
	HALV	0.593 \pm 0.052	HAHV-HALV	-3.537	0.002
	LALV	0.546 \pm 0.048	LAHV-LALV	-0.671	0.507
Diameter	HAHV	0.052 \pm 0.0045	HAHV-LAHV	-5.584	0
	LAHV	0.056 \pm 0.0071	HALV-LALV	-6.942	0
	HALV	0.048 \pm 0.0045	HAHV-HALV	7.448	0
	LALV	0.055 \pm 0.0062	LAHV-LALV	1.048	0.303
Eccentricity	HAHV	0.039 \pm 0.0034	HAHV-LAHV	-5.609	0
	LAHV	0.042 \pm 0.0051	HALV-LALV	-6.848	0
	HALV	0.037 \pm 0.0033	HAHV-HALV	8.096	0
	LALV	0.042 \pm 0.0048	LAHV-LALV	1.148	0.26



$P = 0.000$, $ES = 0.614$], valence conditions [$F(29,1) = 6.548$, $P = 0.016$, $ES = 0.179$] and at interactions between the valence and arousal conditions [$F(29,1) = 5.015$, $P = 0.033$, $ES = 0.143$]. Additionally, there were significant differences in Degree_{max} under arousal conditions [$F(29,1) = 58.569$, $P = 0.000$, $ES = 0.611$], valence conditions [$F(29,1) = 29.718$, $P = 0.000$, $ES = 0.498$] and the interaction between the valence and arousal conditions [$F(29,1) = 4.423$, $P = 0.044$, $ES = 0.128$]. Furthermore, there were significant differences in leaf fraction under arousal conditions [$F(29,1) = 29.169$, $P = 0.000$, $ES = 0.493$], valence conditions [$F(29,1) = 7.48$, $P = 0.01$, $ES = 0.2$] and the interaction between valence and arousal conditions [$F(29,1) = 4.443$, $P = 0.043$, $ES = 0.129$]. Meanwhile, there are also significant differences in the diameter and eccentricity of the minimum spanning tree. Diameter characteristics are given for arousal conditions [$F(29,1) = 67.076$, $P = 0.000$, $ES = 0.691$], valence conditions [$F(29,1) = 14.23$, $P = 0.001$, $ES = 0.322$] and for the interaction between valence and arousal conditions [$F(29,1) = 4.478$, $P = 0.043$, $ES = 0.13$]. Eccentricity characteristics are given for arousal conditions [$F(29,1) = 63.574$, $P = 0.000$, $ES = 0.679$], valence conditions [$F(29,1) = 15.937$, $P = 0.000$, $ES = 0.347$] and the interaction between valence and arousal conditions [$F(29,1) = 5.213$, $P = 0.03$, $ES = 0.148$].

In order to explore the interaction between valence and arousal, a paired t -test and an FDR correction was carried out for

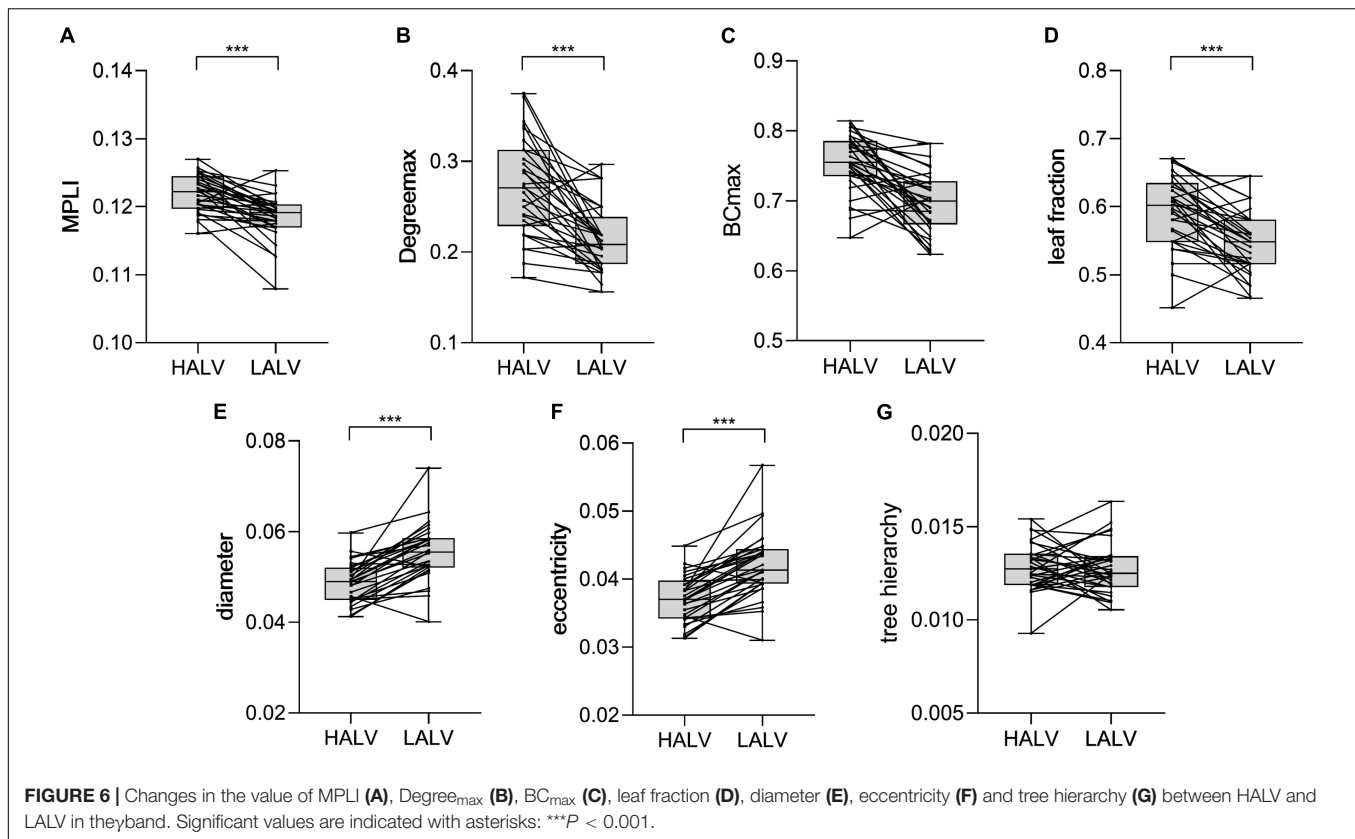
the characteristic values with significant differences in interaction between valence and arousal.

Statistical Analysis Results for HAHV and LAHV

The comparison results show that the MST characteristics of Degree_{max} ($P = 0.000$, $t = 6.241$), leaf fraction ($P = 0.016$, $t = 2.594$), diameter ($P = 0.000$, $t = -5.584$), eccentricity ($P = 0.000$, $t = -5.609$) and MPLI ($P = 0.036$, $t = 2.326$) had significant differences (Table 3). The values of MPLI, Degree_{max} and leaf fraction were higher for HAHV than for LAHV, but the values of eccentricity and diameter were lower for HAHV than for LAHV (Figure 5).

Statistical Analysis Results for HALV and LALV

The comparison results showed that there were significant differences in the MST characteristics (Table 3). Degree_{max} ($P = 0.000$, $t = 5.903$), leaf fraction ($P = 0.001$, $t = 5.218$), diameter ($P = 0.000$, $t = -6.942$), eccentricity ($P = 0.000$, $t = -6.848$) and MPLI ($P = 0.000$, $t = 5.572$). The MPLI, Degree_{max} and leaf fraction values were higher for HALV than for LALV, but the eccentricity and diameter values were lower for HALV than for LALV (Figure 6).



Statistical Analysis Results for HAHV and HALV

The comparison results show that the MST characteristics Degree_{max} ($P = 0.000$, $t = -4.467$), leaf fraction ($P = 0.002$, $t = -3.537$), diameter ($P = 0.000$, $t = 7.448$), eccentricity ($P = 0.000$, $t = 8.096$) and MPLI ($P = 0.000$, $t = -4.752$) had significant differences (Table 3). The MPLI, Degree_{max} and leaf fraction values for HALV were higher than for HAHV, but the eccentricity and diameter values for HALV were lower than for HAHV (Figure 7).

Statistical Analysis Results for LAHV and LALV

The comparison results show that the MST characteristic Degree_{max} ($P = 0.026$, $t = -2.367$) had significant differences (Table 3). The comparison results of LAHV and LALV in the γ band show that the Degree_{max} of LALV were larger than those of LAHV (Figure 8).

The Distribution of Hub Nodes in the MST

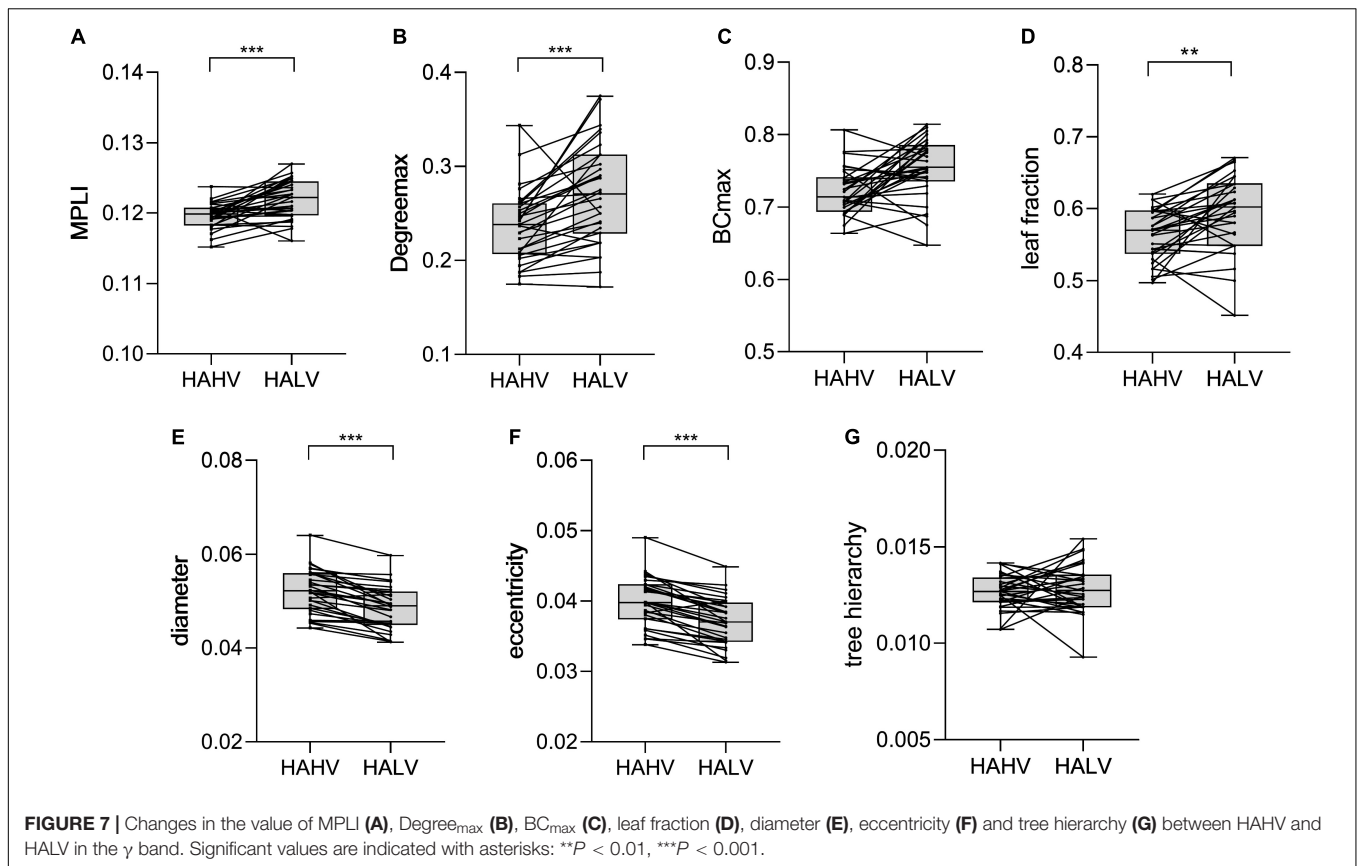
Some interesting findings emerged from studying the topology of the MST. The topological structure of the mean MST represents the structure of the minimum spanning tree of the brain network of most subjects under a certain emotion. The large node degrees in an average MST represent that most of the minimum spanning trees have connections in these nodes, which can reflect whether

the brain network is active (Table 4). In the γ band, the hub nodes of the MSTs for different emotions were distributed across different brain regions (Figure 3). In the MST of HAHV, the hub nodes were mainly concentrated in the frontal lobe area (FP1, FC5) and temporal lobe (T7, T8). The hub nodes in the MST of HALV were mainly concentrated in the frontal lobe (FP2), occipital area (O2) and temporal lobe (T8). The hub nodes in the MST of LAHV were mainly concentrated in the frontal area (FP1, FC5). The hub nodes in the MST of LALV were mainly concentrated in the central parietal (CP5, CP6) and temporal lobe areas (T7).

DISCUSSION

There are significant differences in network characteristics between HAHV and LAHV, HALV and LALV, and HAHV and HALV in the γ band. In other recent research related to emotion, significant differences were also mainly concentrated in the γ band (Mu et al., 2017; Batashvili et al., 2019). In addition, recent studies on emotion classifiers have found that the γ band provides the highest classification accuracy of any frequency band (Mohammadi et al., 2017).

Many studies have also found that the frontal, temporal, parietal and occipital areas of the brain are related to emotional processing from the perspectives of MRI and EEG (Guntekin and Basar, 2007; Ma et al., 2012; Aydin et al., 2018; Zheng et al., 2019). This concept is consistent with our research showing that the

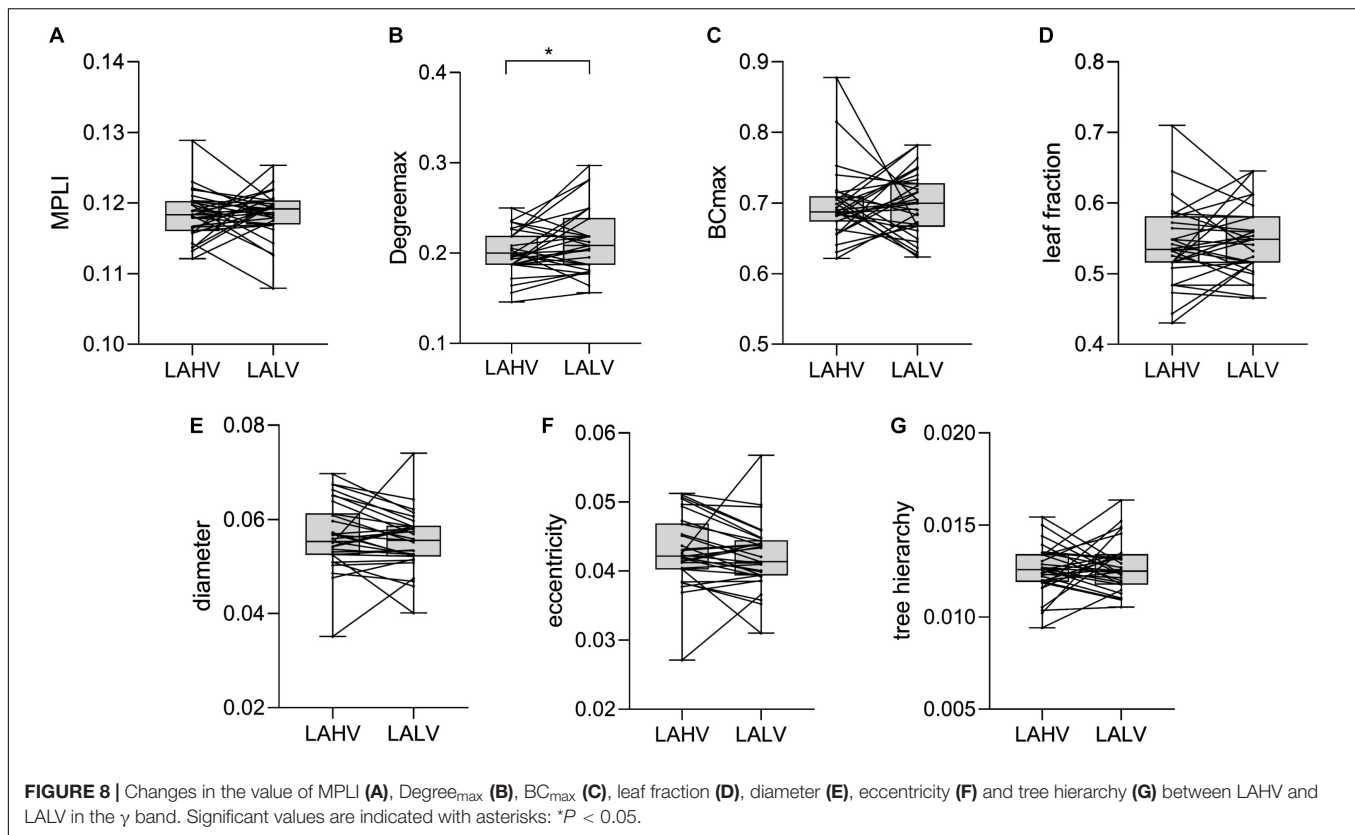


hub nodes of the MST are concentrated in the frontal, temporal, parietal and occipital areas.

Under the same high valence level, HAHV showed a significant higher MPLI than LAHV. MPLI represents the average connection strength of different brain regions during different emotional stimuli. The average connection strength of the brain network is greater for HAHV than for LAHV, implying that, under the same high valence of stimulation, high arousal can stimulate greater brain activity than low arousal. HAHV showed a significant higher leaf fraction than LAHV, while HAHV showed significant lower diameter and eccentricity than LAHV. A large leaf fraction indicates that many leaf nodes exist in the MST network, and the network tends to have a star-shaped topology. In networks with many leaf nodes, the key routes of information flow converge at one or a few hub nodes. Therefore, the BC_{max} and Degree_{max} values of these hub nodes are large. Our results are consistent with the above: HAHV showed significant higher Degree_{max} and leaf fraction than LAHV. Eccentricity is a local node characteristic. Nodes with low eccentricity are central nodes. The smaller the eccentricity value of a node, the closer the node is to the central node location. When the average eccentricity of an MST is small, the topological structure of the MST tends to be star-shaped. Diameter is the longest path between any two nodes in the MST. A decrease in diameter means that the number of leaves increases, which further shows that the topology of the MST tends to be star-shaped. The star topological structure corresponds to a random brain network (Figure 2).

Consequently, the MST topology of HAHV showed more star-shaped configuration than that of LAHV, which indicates that a high-arousal network has more random connections than a low-arousal network. A study by Varotto found that in normal subjects, pleasant music caused an increase in the number of brain network connections compared to a resting state (Varotto et al., 2012). In other words, their results are consistent with ours.

Under the same low valence level, HALV showed a significant higher MPLI than LALV, indicating that the average connection strength of the brain is greater for HALV than for LALV. Under the same low valence, high arousal can stimulate the brain more actively than low arousal, which is consistent with the above conclusion. HALV showed significant higher Degree_{max} and leaf fraction than LALV, while HALV showed significant lower diameter and eccentricity than LALV. This result indicated that the MST topology of HALV showed a more star-shaped configuration than that of LALV. At this time, the values of BC_{max} and Degree_{max} of hub nodes also increased with arousal. As confirmed by our results, HALV showed a significant higher Degree_{max} than LALV. Meanwhile, HALV showed significant lower eccentricity and diameter than LALV, which further shows that the topological structure of HALV is closer to a star configuration. Compared to the brain network associated with LALV, the increase toward randomness of brain network associated with HALV can be proven. In general, a high-arousal brain network has more random connections than does a low-arousal brain network. Nicola Martini et al. also found



a difference in phase synchronization between unpleasant and neutral stimuli in the γ band (Martini et al., 2012). The studies of Balconi and Lucchiari showed that compared with low arousal (sadness), high arousal (anger and fear) increased the brain's γ activity (Balconi and Lucchiari, 2008). Miskovic found that EEG coherence increased when subjects viewed high-arousal pictures (Miskovic and Schmidt, 2010).

Chanel found that the emotion of valence is more difficult to recognize than that of arousal, which supports the view that the correlation between physiological signals and arousal is better than that of valence (Chanel et al., 2009). As discussed earlier, in the comparison of arousal, there were significant differences among different levels of arousal in the same valence level. However, when compared with different valence aspects at the same arousal level, there was little significant difference in characteristics between LAHV and LALV. A possible explanation is that the low arousal and emotional activation of LAHV and LALV resulted in no significant characteristic difference.

Interestingly, there were significant differences in MPLI and MST characteristics between HAHV and HALV. Initially, HALV showed a significant higher MPLI than HAHV and it indicated the average connection strength of the brain network was greater in HALV than in HAHV. Brain activation is higher and more information is transmitted between brain regions in a low-valence emotion than in a high-valence emotion. The brain response to HALV (anger and shocked) stimulation is stronger compared with HAHV (happy and excited) stimulation. Meanwhile, HALV showed significant higher Degree_{max} and

leaf fraction than HAHV and significant lower diameter and eccentricity than HAHV. This result indicated that the MST topology of HALV showed more star-shaped configuration than that of HAHV. HAHV showed significant higher eccentricity and diameter than HALV, which further illustrated that the MST topology of HAHV showed a more line-shaped configuration than that of HALV. From the perspective of a brain network, there are more random connections between brain regions and the development of the brain network structure tends toward randomization in a HAHV brain network compared to a HALV brain network. Consistent with our findings, Ma also found that the characteristic path length of the brain network for negative emotions is longer than that of positive emotions. A short characteristic path represents random connection increases in the

TABLE 4 | Nodes with an average minimum spanning tree degree in the γ band greater than or equal to 3.

HAHV	HALV	LAHV	LALV
T7 ($k = 9$)	FP2 ($k = 5$)	FP1 ($k = 4$)	FC5 ($k = 7$)
FC5 ($k = 5$)	T8 ($k = 5$)	FC5 ($k = 4$)	T7 ($k = 5$)
FP1 ($k = 4$)	O2 ($k = 4$)	CP6 ($k = 4$)	FP1 ($k = 4$)
T8 ($k = 4$)	FP1 ($k = 3$)	F3 ($k = 3$)	CP5 ($k = 4$)
FP2 ($k = 3$)	FC5 ($k = 3$)	T7 ($k = 3$)	CP6 ($k = 4$)
Fz ($k = 3$)	FC6 ($k = 3$)	F4 ($k = 3$)	Pz ($k = 3$)
	P8 ($k = 3$)	F8 ($k = 3$)	P8 ($k = 3$)
		C4 ($k = 3$)	

brain network. That means when the brain deals with negative emotions, brain regions are more activated (Ma et al., 2012).

CONCLUSION

The results show that there are significant differences in MPLI and MST characteristics among different emotions in the γ band. From the perspective of the MST, high-arousal trees showed a more star-shaped configuration than low-arousal trees. However, the low-valence tree showed a more star-shaped configuration than the high-valence tree in the same high arousal level. This result indicated that the brain networks for low-valence states had a more random topological structure and more connections between brain regions than the brain networks of high-valence states. This study provides theoretical support for research on negative bias.

DATA AVAILABILITY STATEMENT

The datasets for this study can be found in the DEAP (<http://www.eecs.qmul.ac.uk/mmv/datasets/deap/>).

REFERENCES

- Amrisha, V., Amanda, W., and Tobias, G. (2008). Not all emotions are created equal: the negativity bias in social-emotional development. *Psychol. Bull.* 134, 383–403. doi: 10.1037/0033-2909.134.3.383
- Aydin, S., Demirtas, S., and Yetkin, S. (2018). Cortical correlations in wavelet domain for estimation of emotional dysfunctions. *Neural Comput. Appl.* 30, 1085–1094. doi: 10.1007/s00521-016-2731-8
- Balconi, M., and Lucchiari, C. (2008). Consciousness and arousal effects on emotional face processing as revealed by brain oscillations. A gamma band analysis. *Int. J. Psychophysiol.* 67, 41–46. doi: 10.1016/j.ijpsycho.2007.10.002
- Batashvili, M., Staples, P. A., Baker, I., and Sheffield, D. (2019). Exploring the relationship between gamma-band activity and maths anxiety. *Cogn. Emot.* 1–11. doi: 10.1080/02699931.2019.1590317 [Online ahead of print]
- Baumeister, R. F., Bratslavsky, E., and Finkenauer, C. (2001). Bad is stronger than good. *Rev. Gen. Psychol.* 5, 323–370. doi: 10.1037/1089-2680.5.4.323
- Boersma, M., Smit, D. J. A., Boomsma, D. I., De Geus, E. J. C., Delemarre-van de Waal, H. A., and Stam, C. J. (2013). Growing trees in child brains: graph theoretical analysis of electroencephalography-derived minimum spanning tree in 5- and 7-year-old children reflects brain maturation. *Brain Connect.* 3, 50–60. doi: 10.1089/brain.2012.0106
- Calhoun, V. D., Wu, L., Allen, E. A., Eichele, T., and Damaraju, E. (2018). EEG signatures of dynamic functional network connectivity states. *Brain Topogr.* 31, 101–116.
- Chanel, G., Kierkels, J. J. M., Soleymani, M., and Pun, T. (2009). Short-term emotion assessment in a recall paradigm. *Int. J. Hum. Comput. Stud.* 67, 607–627. doi: 10.1016/j.ijhcs.2009.03.005
- Demuru, M., Fara, F., and Fraschini, M. (2013). Brain network analysis of EEG functional connectivity during imagery hand movements. *J. Integr. Neurosci.* 12, 441–447. doi: 10.1142/s021963521350026x
- Eric, V. D., Sander, J. H., Diederer, K., Braun, P. J., Floor, E. J., and Stam, C. J. (2013). Functional and structural brain networks in epilepsy: what have we learned? *Epilepsia* 11, 1855–1865. doi: 10.1111/epi.12350
- Fellinger, R., Klimesch, W., Schnakers, C., Perrin, F., Freunberger, R., Gruber, W., et al. (2011). Cognitive processes in disorders of consciousness as revealed by

ETHICS STATEMENT

Ethical review and approval was not required for the study on human participants in accordance with the local legislation and institutional requirements. The patients/participants provided their written informed consent to participate in this study.

AUTHOR CONTRIBUTIONS

RC designed the research and developed the method. YH analyzed the data with the support of HS and SH. YH wrote the first draft of the manuscript, which all authors revised and approved. XW and YG provide help in algorithms and programs, as well as in the use of professional software. RC directed the study. All authors participated to the scientific discussion.

FUNDING

This project is supported by the National Natural Science Foundation of China (61672374 and 61873178), the Natural Science Foundation of Shanxi (201801D121135 and 201901D111093) and the International Science and Technology Cooperation Project of Shanxi (201803D421047).

- EEG time-frequency analyses. *Clin. Neurophysiol.* 122, 2177–2184. doi: 10.1016/j.clinph.2011.03.004
- Fraschini, M., Demuru, M., Crobe, A., Marrosu, F., Stam, C. J., and Hillebrand, A. (2016). The effect of epoch length on estimated EEG functional connectivity and brain network organisation. *J. Neural Eng.* 13:10. doi: 10.1088/1741-2560/13/3/036015
- Groppe, D. M., Bickel, S., Keller, C. J., Jain, S. K., Hwang, S. T., Harden, C., et al. (2013). Dominant frequencies of resting human brain activity as measured by the electrocorticogram. *Neuroimage* 79, 223–233. doi: 10.1016/j.neuroimage.2013.04.044
- Guntekin, B., and Basar, E. (2007). Emotional face expressions are differentiated with brain oscillations. *Int. J. Psychophysiol.* 64, 91–100. doi: 10.1016/j.ijpsycho.2006.07.003
- Koelstra, S., Muhl, C., Soleymani, M., Lee, J. S., Yazdani, A., Ebrahimi, T., et al. (2012). DEAP: a database for emotion analysis using physiological signals. *IEEE Trans. Affect. Comput.* 3, 18–31. doi: 10.1109/t-affc.2011.15
- Kruskal, J. B. (1956). On the shortest spanning subtree of a graph and the traveling salesman problem. *Proc. Am. Math. Soc.* 7, 48–51. doi: 10.2307/2033241
- Kuai, H. Z., Xu, H. X., and Yan, J. Z. (2017). “Emotion recognition from EEG using rhythm synchronization patterns with joint time-frequency-space correlation,” in *Brain Informatics: International Conference*, eds Z. Yi and H. Yong (Beijing: Springer International), 159–168. doi: 10.1007/978-3-319-70772-3
- Li, Y. J., Cao, D., Wei, L., Tang, Y. Y., and Wang, J. J. (2015). Abnormal functional connectivity of EEG gamma band in patients with depression during emotional face processing. *Clin. Neurophysiol.* 126, 2078–2089. doi: 10.1016/j.clinph.2014.12.026
- Liu, S., Tong, J. J., Meng, J. Y., Yang, J. J., Zhao, X., He, F., et al. (2018). Study on an effective cross-stimulus emotion recognition model using EEGs based on feature selection and support vector machine. *Int. J. Mach. Learn. Cybernet.* 9, 721–726. doi: 10.1007/s13042-016-0601-4
- Ma, M., Li, Y., Xu, Z., Tang, Y., and Wang, J. (2012). “Small-world network organization of functional connectivity of EEG gamma oscillation during emotion-related processing,” in *Proceedings of the 2012 5th International Conference On Biomedical Engineering And Informatics*, (Chongqing: IEEE), 16–18. doi: 10.1109/BMEI.2012.6513195

- Martini, N., Menicucci, D., Sebastiani, L., Bedini, R., Pingitore, A., Vanello, N., et al. (2012). The dynamics of EEG gamma responses to unpleasant visual stimuli: from local activity to functional connectivity. *Neuroimage* 60, 922–932. doi: 10.1016/j.neuroimage.2012.01.060
- Miskovic, V., and Schmidt, L. A. (2010). Cross-regional cortical synchronization during affective image viewing. *Brain Res.* 1362, 102–111. doi: 10.1016/j.brainres.2010.09.102
- Mohammadi, Z., Frounchi, J., and Amiri, M. (2017). Wavelet-based emotion recognition system using EEG signal. *Neural Comput. Appl.* 28, 1985–1990. doi: 10.1007/s00521-015-2149-8
- Mu, Y., Han, S. H., and Gelfand, M. J. (2017). The role of gamma interbrain synchrony in social coordination when humans face territorial threats. *Soc. Cogn. Affect. Neurosci.* 12, 1614–1623. doi: 10.1093/scan/nsx093
- Olofsson, J. K., Nordin, S., Sequeira, H., and Polich, J. (2008). Affective picture processing: an integrative review of ERP findings. *Biol. Psychol.* 77, 247–265. doi: 10.1016/j.biopsycho.2007.11.006
- Pegg, S., Dickey, L., Mumper, E., Kessel, E., Klein, D. N., and Kujawa, A. (2019). Stability and change in emotional processing across development: a 6-year longitudinal investigation using event-related potentials. *Psychophysiology* 56:19. doi: 10.1111/psyp.13438
- Rubinov, M., and Sporns, O. (2010). Complex network measures of brain connectivity: uses and interpretations. *Neuroimage* 52, 1059–1069. doi: 10.1016/j.neuroimage.2009.10.003
- Stam, C. J., Nolte, G., and Daffertshofer, A. (2007). Phase lag index: assessment of functional connectivity from multi channel EEG and MEG with diminished bias from common sources. *Hum. Brain Mapp.* 28, 1178–1193. doi: 10.1002/hbm.20346
- Stam, C. J., Tewarie, P., Van Dellen, E., van Straaten, E. C. W., Hillebrand, A., and Van Mieghem, P. (2014). The trees and the forest: characterization of complex brain networks with minimum spanning trees. *Int. J. Psychophysiol.* 92, 129–138. doi: 10.1016/j.ijpsycho.2014.04.001
- Tewarie, P., Hillebrand, A., Schoonheim, M. M., van Dijk, B. W., Geurts, J. J. G., Barkhof, F., et al. (2014). Functional brain network analysis using minimum spanning trees in Multiple Sclerosis: an MEG source-space study. *Neuroimage* 88, 308–318. doi: 10.1016/j.neuroimage.2013.10.022
- Tewarie, P., van Dellen, E., Hillebrand, A., and Stam, C. J. (2015). The minimum spanning tree: an unbiased method for brain network analysis. *Neuroimage* 104, 177–188. doi: 10.1016/j.neuroimage.2014.10.015
- Tijms, B. M., Wink, A. M., de Haan, W., van der Flier, W. M., Stam, C. J., Scheltens, P., et al. (2013). Alzheimer's disease: connecting findings from graph theoretical studies of brain networks. *Neurobiol. Aging* 34, 2023–2036. doi: 10.1016/j.neurobiolaging.2013.02.020
- van Dellen, E., Douw, L., Hillebrand, A., Hamer, P. C. D., Baayen, J. C., Heimans, J. J., et al. (2014). Epilepsy surgery outcome and functional network alterations in longitudinal MEG: a minimum spanning tree analysis. *Neuroimage* 86, 354–363. doi: 10.1016/j.neuroimage.2013.10.010
- van Diessen, E., Numan, T., van Dellen, E., van der Kooi, A. W., Boersma, M., Hofman, D., et al. (2015). Opportunities and methodological challenges in EEG and MEG resting state functional brain network research. *Clin. Neurophysiol.* 126, 1468–1481. doi: 10.1016/j.clinph.2014.11.018
- van Diessen, E., Otte, W. M., Stam, C. J., Braun, K. P. J., and Jansen, F. E. (2016). Electroencephalography based functional networks in newly diagnosed childhood epilepsies. *Clin. Neurophysiol.* 127, 2325–2332. doi: 10.1016/j.clinph.2016.03.015
- van Wijk, B. C. M., Stam, C. J., and Daffertshofer, A. (2010). Comparing brain networks of different size and connectivity density using graph theory. *PLoS One* 5:e13710. doi: 10.1371/journal.pone.0013701
- Varotto, G., Fazio, P., Sebastiano, D. R., Avanzini, G., Franceschetti, S., Panzica, F., et al. (2012). “Music and Emotion: an EEG connectivity study in patients with disorders of consciousness,” in *Proceedings of the 2012 Annual International Conference of the Ieee Engineering in Medicine and Biology Society*, (New York, NY: IEEE), 5206–5209.
- Zhang, D. D., Wang, L. L., Luo, Y., and Luo, Y. J. (2012). Individual differences in detecting rapidly presented fearful faces. *PLoS One* 7:e49517. doi: 10.1371/journal.pone.0049517
- Zheng, W. L., Zhu, J. Y., and Lu, B. L. (2019). Identifying stable patterns over time for emotion recognition from EEG. *IEEE Trans. Affect. Comput.* 10, 417–429. doi: 10.1109/taffc.2017.2712143
- Zhu, L., Lotte, F., Cui, G. C., Li, J. H., Zhou, C. L., and Cichocki, A. (2018). “Neural mechanisms of social emotion perception: an EEG hyper-scanning study,” in *Proceedings of the 2018 International Conference on Cyberworlds*, eds A. Sourin and O. Sourna (Piscataway, NJ: IEEE), 199–206. doi: 10.1109/CW.2018.00045

Conflict of Interest: The authors declare that the research was conducted in the absence of any commercial or financial relationships that could be construed as a potential conflict of interest.

Copyright © 2020 Cao, Hao, Wang, Gao, Shi, Huo, Wang, Guo and Xiang. This is an open-access article distributed under the terms of the Creative Commons Attribution License (CC BY). The use, distribution or reproduction in other forums is permitted, provided the original author(s) and the copyright owner(s) are credited and that the original publication in this journal is cited, in accordance with accepted academic practice. No use, distribution or reproduction is permitted which does not comply with these terms.